

Grain Boundary Migration in Fe–3mass%Si Alloy Bicrystals under a Magnetic Field

Sadahiro TSUREKAWA,¹⁾ Kyosuke INOUE²⁾ and Pavel LEJČEK³⁾

1) Department of Materials Science and Engineering, Graduate School of Science and Technology, Kumamoto University, 2-39-1 Kurokami, Kumamoto 860-8555 Japan. 2) Department of Nanomechanics, Graduate School of Engineering, Tohoku University, Aramaki-aza-Aoba, Aoba-ku, Sendai 980-8579 Japan. 3) Institute of Physics, Academy of Sciences of the Czech Republic, Na Slovance 2, 182 21 Praha 8, Czech Republic.

(Received on October 26, 2009; accepted on February 10, 2010)

Grain boundary migration under a magnetic field was studied using Fe–3mass%Si alloy bicrystals with $\langle 001 \rangle / \Sigma 5$ ($\phi = 36^\circ$) and $\langle 001 \rangle / \text{random}$ ($\phi = 45^\circ$) tilt boundaries at temperatures between 1 223 K and 1 323 K. A capillarity method (Sun and Bauer method) was used to observe grain boundary migration. A 6 T magnetic field was applied parallel to the [100] direction, which is one of easy magnetization directions, in a grain whose area increases with occurring grain boundary migration. It was found that the application of a magnetic field observably increased the velocity of grain boundary migration for both bicrystals. The abrupt change in the velocity of grain boundary migration was observed at a critical capillary driving force irrespective of whether the magnetic field was applied. However, this critical driving force was decreased by application of a magnetic field. It was suggested that the magnetic field act as a driving force for grain boundary migration rather than increase its mobility.

KEY WORDS: grain boundary migration; magnetic field; grain boundary character; Fe–Si alloy; bicrystal.

1. Introduction

Mechanical and functional properties of the polycrystalline materials are significantly influenced by microstructure, and the microstructure can change variedly with processing routes of materials.¹⁾ Recently, the usefulness of application of a magnetic field during materials processing has been increasingly recognized in microstructural control of not only metallic materials but also ceramic ones.²⁾ Since Pender and Jones have reported in 1913 that a fine and homogeneous pearlite structure could be achieved by applying alternating magnetic field during phase transformation,³⁾ extensive studies have evidenced that a magnetic field exerts significant influences on metallurgical phenomena.^{4,5)} For instance, enhancement of grain growth and homogeneity in grain size distribution were found to be promoted by application of a magnetic field in nanocrystalline nickel⁶⁾ and carbonyl iron compact.⁷⁾ Because grain boundary migration is indispensable to the phenomena, such as recrystallization and grain growth, related to the development of microstructure in polycrystalline materials, it is essential to study grain boundary migration in a magnetic field for clarifying the origin of the magnetic field effect on the microstructure evolution. As for the influence of the magnetic field on the grain boundary migration, Mullins⁸⁾ has first performed experiments with a diamagnetic bismuth polycrystal and discussed on the driving force arising from magnetic anisotropy. Later, bicrystal studies have been conducted using bismuth^{9,10)} and zinc,¹¹⁾ and demonstrated that

the energy associated with magnetic anisotropy can drive grain boundary migration. However, there are few studies on grain boundary migration in a magnetic field for ferromagnetic materials with a potential applied to electromagnetic processing. One of the authors (S.T.) has reported that the influence of a magnetic field on grain boundary migration of Fe–2.5mass%Si bicrystal and showed that a magnetic field increased the grain boundary migration velocity.¹²⁾ In the present paper, a further systematic investigation was made to obtain comprehensive knowledge as to grain boundary migration of an Fe–Si alloy bicrystal in a magnetic field.

2. Experimental Procedures

2.1. Preparation of Bicrystals

It is well known that the mobility of grain boundary migration depends on its character. We prepared Fe–3mass% Si bicrystals with $\langle 001 \rangle / \Sigma 5$ ($\phi = 36^\circ$) and $\langle 001 \rangle / \text{random}$ ($\phi = 45^\circ$) symmetric tilt boundaries by a floating zone technique. The cylindrical bicrystals were cut into slices of 1.3 mm in thickness so as for the surface orientation of the samples to be {001}. Furthermore, these samples were cut into such a rectangular shape with dimensions of 8.0 mm \times 3.7 mm that the grain boundary made a contact angle of α with the edge of the sample to be approximately 20° as shown in **Fig. 1**, and then mechanically ground to No. 4000 emery paper and buff-polished into mirror surface using Al_2O_3 slurry and colloidal silica. Thereafter, they were an-

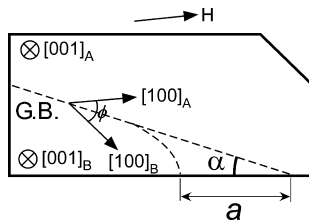


Fig. 1. Illustration for the Sun and Bauer method and grain boundary geometry used in this study.

nealed at 1070 K for 21.6 ks under a vacuum of 1.0×10^{-3} Pa to remove strain probably introduced during the sample preparation.

2.2. Grain Boundary Migration in a Magnetic Field

A capillarity method (Sun–Bauer method¹³) was applied to observe grain boundary migration. Figure 1 illustrates the Sun and Bauer method and grain boundary geometry used in this study. The grain boundary migrates to decrease the area of the grain boundary by the capillary force. The capillary force P as the driving force for the grain boundary migration is given by,

$$P = \kappa\gamma \dots\dots\dots(1)$$

where κ is a curvature of the migrating grain boundary, and γ grain boundary energy. At the side surface of the sample, the curvature κ is given by,

$$\kappa = \frac{f(\alpha)}{a(t)} \dots\dots\dots(2)$$

where $f(\alpha)$ is the geometric factor as a function of α , which is the angle between original planar boundary and the side surface of the sample, and $a(t)$ the displacement of the grain boundary. The value of $f(\alpha)$ was theoretically calculated as a function of α ,^{13,14} and experimentally obtained as the ratio between the displacement of grain boundary and the radius of grain boundary curvature at the side surface of the sample according to Eq. (2), as exemplified in Fig. 2. The values of $f(\alpha)$ experimentally obtained is in good agreement with the theoretically calculated ones.¹⁴ Consequently, the velocity of grain boundary migration v is obtained as follows:

$$v = \frac{da(t)}{dt} = M\gamma\kappa = M\gamma \frac{f(\alpha)}{a(t)} \dots\dots\dots(3)$$

where, M is the mobility of grain boundary migration. Therefore, the relation between displacement, $a(t)$, of the grain boundary along the side surface and time, t , is described by,

$$a(t)^2 = kt, \quad k = 2M\gamma f(\alpha) \dots\dots\dots(4)$$

A 6 T magnetic field was applied parallel to the [100] direction, which is one of easy magnetization directions, in a grain whose area increases with occurring grain boundary migration, as shown by the arrow in Fig. 1. Under these conditions, we investigated whether or not a magnetic field could assist grain boundary migration by acting as excess driving force in addition to the capillary driving force.

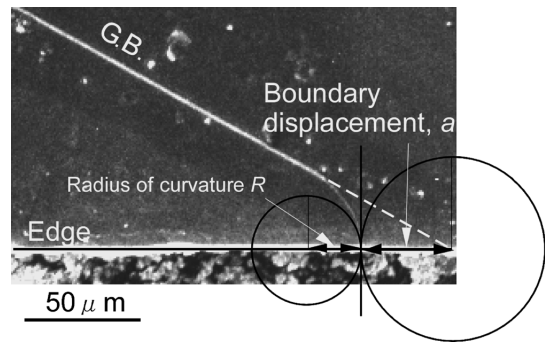


Fig. 2. Determination of the geometric factor, $f(\alpha)$, from the displacement and the radius of curvature of the migrating grain boundary.

Bicrystal samples were annealed at temperatures ranging from 1 223 to 1 323 K in the paramagnetic temperature region, where the displacement of the grain boundary migration could be observed, with a 6 T magnetic field and without a magnetic field. After annealing for a specific time, the position of the grain boundary was observed by using an automated SEM/EBSD, and then the displacement was measured. By repeating this procedure, relation between the displacement of grain boundary migration and time was obtained. The SEM/EBSD observations were made with a Hitachi S-4200 FEG-SEM, equipped with an OIM system from TSL, operating at a 20 kV accelerating voltage.

3. Results and Discussion

3.1 Relation between Grain Boundary Migration Distance and Time

Figure 3 represents series of EBSD/OIM micrographs showing migration of random and $\Sigma 5$ grain boundaries at 1 273 K (a) in a 6 T magnetic field and (b) in a non-magnetic field. The arrows in this figure indicate the initial position of the grain boundaries at the edge of the samples. We can see that the grain boundary migrate towards the left-hand side along the edge of the sample. From such a series of observations, the square of boundary displacement was plotted against time, according to Eq. (4). Figure 4 shows the relation between them for $\Sigma 5$ and random grain boundaries at 1 273 K without and with 6 T magnetic field. To correct the difference in capillary driving force depending on the angle α , the square of the boundary displacement was normalized by $f(\alpha)$. The square of boundary displacement is found to be a linear function of time. Of particular interest is the finding that grain boundary migration can be enhanced by application of the magnetic field, irrespective of grain boundary character.

3.2. Temperature Dependence of Grain Boundary Mobility

Figure 5 shows the Arrhenius plot of the product of the grain boundary mobility and grain boundary energy, $M\gamma$. In this figure, $\Sigma 5$ and random boundaries are displayed by the broken-line and solid line, respectively. The activation energy for grain boundary migration calculated from Fig. 5 is ranging from 700 to 1 400 kJ/mol. The activation energy obtained seems to be higher for random boundary than for $\Sigma 5$ boundary. However, these values are much higher than

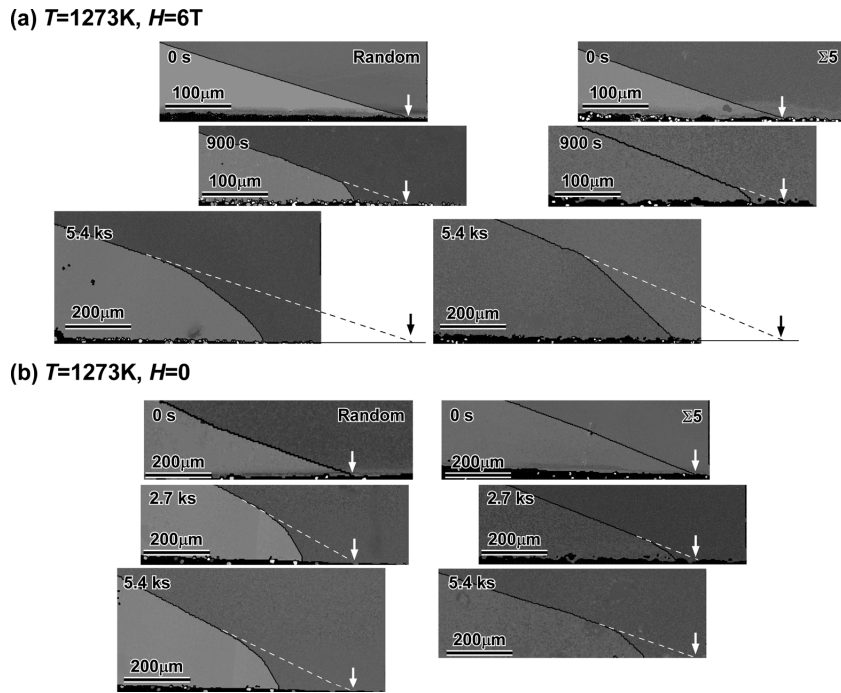


Fig. 3. Series of EBSD/OIM micrographs showing grain boundary migration of random and $\Sigma 5$ boundaries at 1273 K (a) in a 6 T magnetic field and (b) in a non-magnetic field. The arrows in this figure indicate the initial position of the grain boundaries at the edge of the samples.

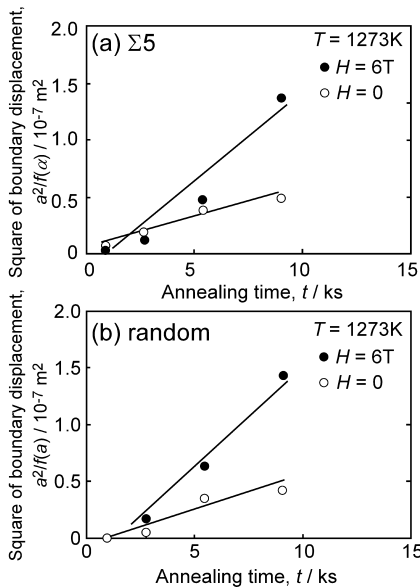


Fig. 4. Changes in the square of boundary displacement with time at 1273 K without and with a 6 T magnetic field for (a) $\Sigma 5$ boundary and (b) random boundary.

activation energies for self-diffusion of iron (240 kJ/mol¹⁵) and for intrinsic diffusion of silicon in iron (220 kJ/mol¹⁶). The reason how come such significantly large activation energies were obtained will be discussed below.

3.3. Dependence of Driving Force on Grain Boundary Migration Velocity

Figure 6 represents the relation between grain boundary migration velocity v and the curvature κ of the grain boundary measured at the sample edge. The capillary driving force is proportional to this curvature as described in Sec. 2.2. The migration velocity of the grain boundary was evaluated from the tangent to the displacement curve plot-

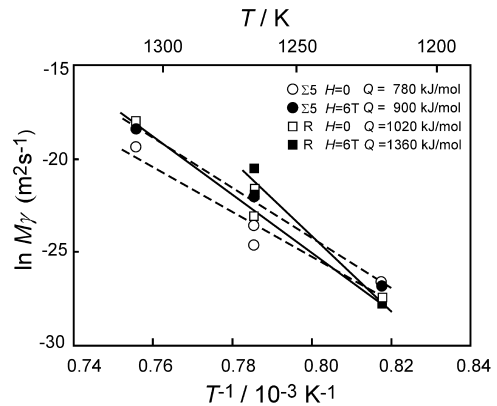


Fig. 5. Temperature dependence of the migration mobility for $\Sigma 5$ and random boundaries under a 6 T magnetic field and non-field.

ted against time. The boundary curvature was evaluated on the basis of Eq. (2). We can see that the grain boundary migration velocity drastically changes at a critical capillary driving force, and the critical driving force decreases with increasing temperature. In addition, the critical driving force is smaller for $\Sigma 5$ grain boundary than for random boundary, and it decreased with application of a 6 T magnetic field. This finding suggests that the mechanism of the grain boundary migration changes according to driving force. Such abrupt change in migration velocity with driving force has been found in the migration of $\Sigma 9$ boundary in Fe-3mass%Si alloy bicrystal.^{14,17} It was reported that the grain boundary moved with dragging silicon atom atmosphere at a smaller driving force, while grain boundary migration was governed by grain boundary diffusion of iron at a larger driving force. Moreover, Fig. 6 revealed that the grain boundary migration velocity was increased by applying a magnetic field even at the same capillary driving force. In contrast, since the slope of each line in Fig. 6 ex-

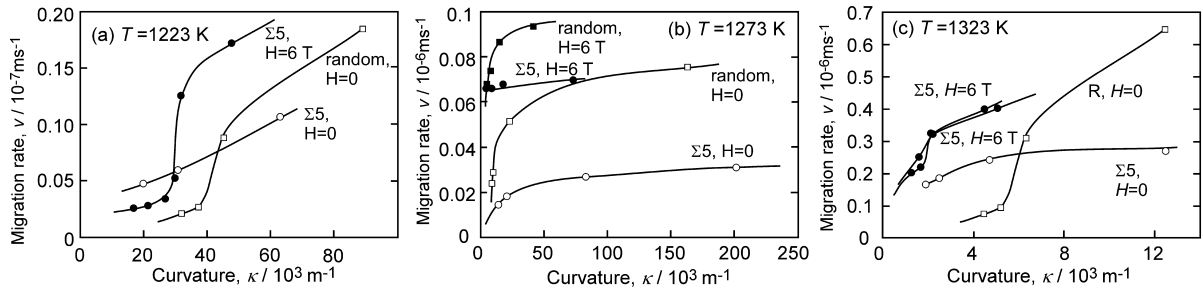


Fig. 6. Changes in migration velocity with the curvature of the grain boundary measured at the specimen edge (the curvature is proportional to driving force) at (a) 1223 K, (b) 1273 K and (c) 1323 K under a 6 T magnetic field and non-field for Σ5 and random boundaries.

cept the regime where the migration velocity drastically changes provides $M\gamma$ as expressed in Eq. (3), there seems to be little difference in the motility of grain boundary migration irrespective of whether a magnetic field is applied. These results suggest that a magnetic field can act as driving force for the grain boundary migration rather than a change in mobility.

As Molodov *et al.* have demonstrated using bismuth bicrystals,^{9,10} magnetic anisotropy energy can drive grain boundary migration. For materials with $|\chi| \ll 1$, where χ is the susceptibility, magnetic driving force due to magnetic anisotropy acting on the boundary of two crystals is given by,

$$p = \frac{\mu_0 H^2}{2} (\chi_1 - \chi_2) \dots\dots\dots(5)$$

where χ_1 and χ_2 are the susceptibilities of crystal 1 and crystal 2, respectively, along the magnetic field H .⁸⁾ Although there is no information about the anisotropy of susceptibility for Fe–Si alloys in paramagnetic state, to the authors’ knowledge, the difference in the susceptibility depending on the crystal orientation is probably small in Fe–Si alloys unlike bismuth. Thus, the driving force due to magnetic anisotropy energy in a magnetic field may be significantly small. The origin of magnetically enhanced grain boundary migration observed has been still unclear for the less anisotropic materials with cubic structure like Fe–Si alloys. In addition to the magnetic anisotropy energy, the magnetostriction might be taken into account as an origin of driving force acting on the boundary under a magnetic field, because magnetostriction may cause a stress concentration around the grain boundary. Recent bicrystal experiments have revealed that a shear stress can promote grain boundary migration.¹⁸⁾ Accordingly, the stress concentration due to magnetostriction is possible to act as a driving force for grain boundary migration.

As mentioned above, the activation energy for grain boundary migration obtained was much larger than those for the intrinsic diffusion of silicon in iron and for the self-diffusion of iron. This is probably because this experiment on grain boundary migration was conducted just in a range of temperatures where the mechanism of grain boundary migration changes. As shown in Fig. 5 and Fig. 7 in the Refs. 17) and 19), respectively, the apparent activation energy for grain boundary migration in the transition temperature regime is evaluated to be considerably large.

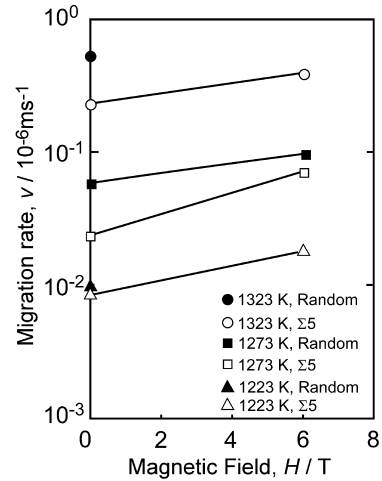


Fig. 7. Dependence of magnetic field strength on grain-boundary migration velocity at a constant capillary force at different temperatures for Σ5 and random boundaries.

3.4. Influence of Magnetic Field on Dependence of Grain Boundary Character on Grain Boundary Migration

Figure 7 shows grain boundary migration rates at a constant capillary driving force as a function of magnetic field strength. It is found that the migration rate increases with increasing magnetic field strength irrespective of grain boundary character. The migration velocity of the random grain boundary is larger than that of the Σ5 grain boundary in both a 6 T magnetic field and non-field. However, the difference between the migration rates of random boundary and Σ5 boundary seems to become small by applying the magnetic field. This finding suggests that the dependence of grain boundary character on grain boundary migration becomes small in a magnetic field, which may be a reason that the application of a magnetic field during annealing often causes homogenization of grain size distribution.^{6,7)}

4. Conclusions

The influence of a magnetic field on grain boundary migration of Fe–3mass%Si alloy bicrystal was studied. The chief results obtained are as follows.

- (1) The grain boundary migration was enhanced by application of a magnetic field, irrespective of grain boundary character.
- (2) Grain boundary migration velocity drastically changes at a critical capillary driving force, and this critical

driving force decreases with increasing temperature and with magnetic field. This abrupt change in migration velocity is probably attributed to change in the mechanism of the grain boundary migration.

(3) The critical capillary driving force was smaller for $\Sigma 5$ grain boundary than for random boundary.

(4) A magnetic field will act as a driving force for grain boundary migration, rather than increase its mobility.

(5) The dependence of grain boundary character on grain boundary migration became small in a magnetic field.

Acknowledgement

The authors would like to express their hearty thanks to Mr. Takashi Matsuzaki (Tohoku University) for his help for experimental work. This work was supported by ISIJ (The Iron and Steel Institute of Japan) Research Promotion Grant, by Grain-in-Aid for Basic Research (S) (Grant No. 19106013) from the JSPS (Japan Society for the Promotion of Science) and by Czech Science Foundation (Grant No. 106/08/0369). These supports are greatly appreciated.

REFERENCES

- 1) T. Watanabe: *Textures Microstruct.*, **20** (1993), 195.
- 2) Proc. of the 5th Int. Symp. on Electromagnetic Processing of Materials (EPM2006), The Iron and Steel Institute of Japan, Tokyo (2006).
- 3) H. Pender and R. L. Jones: *Phys. Rev.*, **1** (1913), 259.
- 4) T. Watanabe, S. Tsurekawa, X. Zhao, L. Zuo and C. Esling: *J. Mater. Sci.*, **41** (2006), 7747.
- 5) T. Watanabe, S. Tsurekawa, X. Zhao and L. Zuo: *Scr. Mater.*, **54** (2006), 969.
- 6) K. Harada, S. Tsurekawa, T. Watanabe and G. Palumbo: *Scr. Mater.*, **49** (2003), 367.
- 7) S. Tsurekawa, K. Harada, T. Sasaki, T. Matsuzaki and T. Watanabe: *Mater. Trans.*, **41** (2000), 991.
- 8) W. W. Mullins: *Acta Metall.*, **4** (1956), 421.
- 9) D. A. Molodov, G. Gottstein, F. Heringhaus and L. S. Shvindlermann: *Scr. Mater.*, **37** (1997), 1207.
- 10) D. A. Molodov, G. Gottstein, F. Heringhaus and L. S. Shvindlermann: *Acta Mater.*, **46** (1998), 5627.
- 11) A. D. Sheikh-Al, D. A. Molodov and H. Garmestani: *Scr. Mater.*, **48** (2003), 483.
- 12) T. Matsuzaki, T. Sasaki, S. Tsurekawa and T. Watanabe: Proc. of 4th Int. Conf. on Recrystallization and Related Phenomena, Japan Institute of Metals, Sendai, (1999), 529.
- 13) R. C. Sun and C. L. Bauer: *Acta Metall.*, **18** (1970), 635.
- 14) H. Nakashima, T. Ueda, S. Tsurekawa, K. Ichikawa and H. Yoshinaga: *Tetsu-to-Hagané*, **82** (1996), 238.
- 15) H. Oikawa: *Tech. Rep., Tohoku Univ.*, **47** (1982), 67.
- 16) H. Oikawa: *Tech. Rep., Tohoku Univ.*, **47** (1982), 215.
- 17) S. Tsurekawa, T. Ueda, K. Ichikawa, H. Nakashima, Y. Yoshitomi and H. Yoshinaga: *Mater. Sci. Forum*, **204–206** (1996), 221.
- 18) D. A. Molodov, T. Gorkaya and G. Gottstein: *Mater. Sci. Forum.*, **558–559** (2007), 927.
- 19) M. Furtkamp, P. Lejček and S. Tsurekawa: *Interface Sci.*, **6** (1998), 56.